frontiers | Frontiers in Ecology and Evolution

TYPE Hypothesis and Theory
PUBLISHED 12 March 2025
DOI 10.3389/fevo.2025.1523532

OPEN ACCESS

EDITED BY
Tian Li,
Nankai University, China

REVIEWED BY
Junfeng Chen,
Qufu Normal University, China
Jayani J. Wewalwela,
University of Colombo, Sri Lanka

*CORRESPONDENCE
Junkang Guo
junkangguo@sust.edu.cn
Gang Yang
yanggang903@163.com

†These authors have contributed equally to this work

RECEIVED 06 November 2024
ACCEPTED 26 February 2025
PUBLISHED 12 March 2025

CITATION
Bai Y, Dai Q, Guo J, Fu W, Yun J, Wang F, Huang J, Zhang R and Yang G (2025) Geobacter abundance in soil regulate by pH and iron-bearing minerals. *Front. Ecol. Evol.* 13:1523532. doi: 10.3389/fevo.2025.1523532

Geobacter abundance in soil regulate by pH and iron-bearing minerals

Yinping Bai[1,2†], Qianli Dai[2†], Junkang Guo[1*], Wei Fu[2], Juanli Yun[1], Fusong Wang[2], Jing Huang[2], Rongping Zhang[2] and Gang Yang[1,2*]

[1]School of Environmental Science and Engineering, Shaanxi University of Science and Technology, Xi'an, China, [2]School of Life Science and Engineering, Southwest University of Science and Technology, Mianyang, China

As an electrogenic bacterium, *Geobacter* plays a crucial role in the geochemical cycles of arable soil. However, little is known about the existence of *Geobacter* and its impact factors in paddy soil and purple soil. We determined *Geobacter* in paddy soil and purple soil in Sichuan Basin, China. The data reveal that soil pH in arable soils is the main factor in determining *Geobacter* abundance, and the coefficient of determination is as high as 72.5%. Iron-bearing minerals (IBM) have a positive relationship with *Geobacter* abundance when their content exceeds 9%. Overall, *Geobacter* abundance in paddy soil is higher than that in purple soil. *Geobacter* in paddy soil prefers acidic environment, whereas *Geobacter* in purple soil prefers neutral environment. *Geobactor* in paddy soil prefers acidic environment, which may be related to long-term irrigation and drainage in paddy fields. In addition, we found that the soil pH in the Sichuan Basin decreased by 0.7 over a period of forty years, providing evidence for the succession of *Geobacter* species in this region that prefer neutral and acidic environments. The acidified soil environment in the Sichuan Basin is conducive to the survival of *Geobacter*. This condition directly influences the iron heterotrophic iron reduction process carried out by *Geobacter* and subsequently impacts soil carbon emissions.

KEYWORDS

arable soil, *Geobacter*, carbon cycles, purple soil, iron-bearing minerals

1 Introduction

Microorganisms in arable soil concurrently govern the soil function including energy regulation, boosting crop yield, strengthening pest and disease resistance, and reducing greenhouse gas emissions (Dubey et al., 2019; Jansson and Hofmockel, 2020; Luo et al., 2018). *Geobacter* is widely distributed in soil and sediment, they have the ability to generate electricity, which can affect on soil carbon, nitrogen, iron, and other elements in soil environment. Because of its unique conductive pili that may carry electrons to insoluble

minerals, electrodes, and other microbes, it plays a significant role in nutrient cycles of arable soil (Li and Zhou, 2020; Lovley et al., 2011; Rotaru et al., 2018). Researches on *geobacter*, include soil environmental remediation, bioenergy conversion, and the sustainable production of green electronics, have led to substantial advancements in biogeochemical soil technology in recent years (Lovley, 2022). The occurrence condition of *Geobacter* in arable soil and its abundance are typically determined by the basic physical and chemical features of the soil (Fierer, 2017). Iron-bearing minerals (IBM) have a function of electron transfer or reduction, which impacts the abundance of *Geobacter* in arable soil (Kato et al., 2012, 2013). Considering the cascading consequences of material and energy cycles in complex and variable arable soil (Methe et al., 2003). Given the role of *Geobacter* in soil biogeochemical cycling, we should have an understanding of the forms and abundance of *Geobacter* present in arable soil. *Geobacter* and *Geothermobacter* are typical genera of the Geobactaceae family. Xu and colleagues have found four new species of Geomonas, which are classified as *Geobacter*aceae and participate in the nitrogen cycle in paddy soil (Xu et al., 2019). 19 identified species have been described for the complete family *Geobacter* (Alikhan et al., 2011). *Geobacter* iron-reducing was found in surface sediments by Lovley. It was first isolated and given the scientific name *Geobacter-metallireducens*(GS-15) (Lovley et al., 1993). Subsequent scientists have identified *Geobacter* sulfurreducens (PCAT), *Geobacter* daltonii (FRC-32T), and *Geobacter* toluenoxdans (TMJ1T) in distinct soil conditions (Caccavo et al., 1994; Kunapuli et al., 2010; Prakash et al., 2010). Since the types of electrons (such as acetate, fumarate, and chloride) required by *Geobacter* for intracellular respiration vary according to changes in soil environmental conditions, the abundance of *Geobacter* in different environmental media also fluctuates (Rengel and Marschner, 2005; Zhu et al., 2022). According to previous research, between 0.26 and 7.70% of the bacteria in the soil of diverse land types have electrogenic function. The majority of *Geobacter* were discovered in the soil around paddy fields and lakes (Wang et al., 2019). It was revealed that longterm fertilization of arable soil did not change *Geobacter* population, however, pH, total carbon (TC), and total nitrogen (TN) in arable soils are regulate bacterium classification differences in the *Geobacter* community (Li et al., 2020). In addition, studies have shown that the addition of IBM can significantly increase the abundance of *Geobacter*. It was reported that the current of the reaction system rose dramatically following the addition of IBM after inoculating paddy soil using the Electrochemical Workstation Culture System, and cloning of 16S rRNA gene segments demonstrated a considerable rise in the abundance of *Geobacter* (Kato et al., 2010). Seasonal changes can also affect the abundance of *Geobacter*. The seasonal changes in the abundance of *Geobacter* are mainly reflected in temperature fluctuations, water levels and crop growth cycles (Kramer et al., 2013; Zheng et al., 2019). The microbial diversity of arable soils varies globally. The Sichuan Basin in China, which produces a substantial quantity of grain crops, has a vast expanse of rich soil and a great number of microbial strain resources (Lei et al., 2022; Wardle et al., 1999). It was determined that *Comamonadaceae* and *Moraxellaceae* were the most frequent bacterial families in arable soil from the Sichuan area. Rhizomicrobium were the predominant bacteria in acidic purple soil (Huang et al., 2013; Li et al., 2021; Liu et al., 2020). According to previous research, *Geobacter* are widely present in rice fields and sediment, and can directly participate in the carbon cycle of rice fields, which is influenced by multiple factors. However, as one of the regions with the highest methane emissions in China, the distribution pattern and influencing factors of *Geobacter*, as well as their impact on methane emissions in the Sichuan Basin, have not been reported yet. In order to explore the relationship between microbial diversity and the environment by gaining a better understanding of the relative abundance and composition of the microbial communities, We used high-throughput 16sRNA sequencing to analyzing the composition and distribution of Geobacter in paddy and purple soil of the Sichuan Basin, China. The objectives of this study were to understand:1) *Geobacter* in arable soils and their controlling factors.2) The effects of IBM on the community and abundance of *Geobacter*.

2 Materials and methods

2.1 Study area and experiment design

The Sichuan Basin is one of the four main basins in China (28° 10′-32°25′N and 101°56′-108°32′E) (Ran and Xinyue, 2018). The Sichuan Basin covers an area of 2.6×10^5 km^2, with an average elevation of 400 m, which is home to around 90 million people. Most of the terrain is composed of plains and hills, with an average annual temperature between 16 and 18 degrees Celsius. This region belongs to the subtropical monsoon climate zone. Most crops planted on arable land are rice, rapeseed, maize, and sweet potatoes. There are several types of arable soil, such as dry field, paddy field (http://ir.imde.ac.cn/: records of Sichuan soil varieties) and according to the second national soil census of China, 77.75% of the soil types in the Sichuan basin are mainly paddy soil and purple soil. We collected soil samples in May and August 2021, respectively, all the sample sites were recored by GPS (Figure 1). 54 samples (0-2 cm) were collected in sterile bags and stored in dry ice boxes, transported to laboratory, and stored in a -80°C freezer. Soil samples at 0-20 cm depth were collected for determination of soil physical and chemical characteristics.

2.2 Soil physical and chemical characteristics analysis

pH was determined by the potentiometric method, with specific steps as follows:weigh 10 g air-dried soil sample, add 25 mL of deionized water (ddH_2O), stir for one minute, and measure after 30 minutes using a pH meter. The Kjeldahl method, the sodium hydroxide melting molybdenum antimony colorimetric method, and the external-heat potassium dichromate oxidation-colorimetric method, with specific operations referring to HJ717-2014, GB8937-

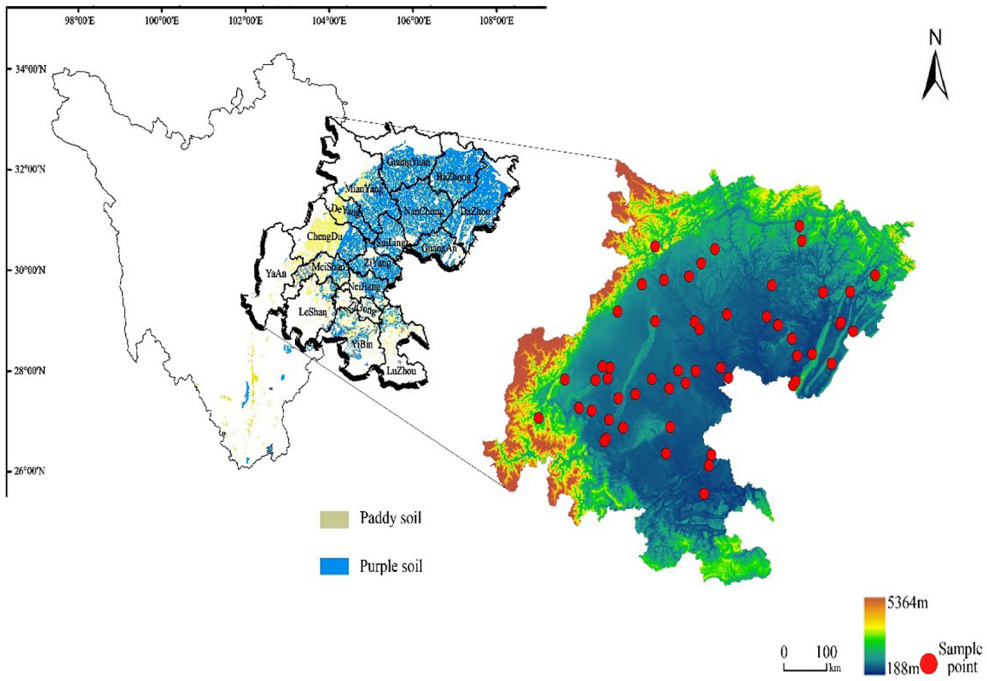

FIGURE 1
Distribution of study area and sampling sites. Sampling sites indicated by red dot from Sichuan Basin, China.

88, and GB9834-1988, were utilized to determine the total nitrogen (TN), total phosphorus (TP), and organic matter (OM) of soil samples. Soil IBM was determined by using an X-ray diffractometer (XRD). A sufficient amount of a sieved 200-mesh sample was used to form an oriented sheet. Then adjust the Cu target to 2.2 kW, working voltage to 60 kV, current to 50 mA, scanning range to 5°–80°, and scanning speed to 5°/min (Harris and Norman White, 2008). IBM's logo appears in the program Jade 9.0. The semi-quantitative XRD "adiabatic method" calculation formula for IBM's mass fraction is as follows: (Chung, 1974):

$$W_x = \frac{I_{xi}}{K_A^x \sum_{i=A}^{N} \frac{I_i}{K_A^i}}$$

(W_x: Mineral phase mass fraction, I: Mineral peak intensity, K: Mineral phase RIR value, $\sum_{i=A}^{N} \frac{I_i}{K_A^i}$: There are N sums of phases I/K).

2.3 Soil DNA extraction and high-throughput sequencing

DNA from soil samples was extracted using a soil DNA kit (BIO101, MP Biomedicals, US). The quantity and molecular size of the extracted DNA were detected by the Nanodrop NC-2000 UV spectrophotometer (Thermo Scientific, USA) and 1.2% agarose gel electrophoresis before further Analysis. The V1-V3 regions of bacterial 16S rRNA gene for PCR amplification. The upper and lower primers are 27F (5'-AGAGTTTGATCCTGGCTCAG-3') and 533R (5'-TTACCGCGGCTGCTGGCAC-3') (Franke-Whittle et al., 2015). The 20 μL reaction mixture includes 0.25 μL of Q5 high-fidelity DNA polymerase, 5 μL of Q5 reaction buffer, 5 μL of Q5 high GC buffer, 10 μL of dNTP (10mM), 2 μL of DNA template, 1 μL of forward and reverse primers (10mM), and 8.75 μL of ddH_2O. The thermal cycling reaction is as follow: After preparing the necessary components for the PCR reaction, the PCR machine performs a 30-second Pre-denaturation at 98°C to thoroughly denature the template DNA before beginning the amplification cycle. In each cycle, the template was denatured by holding it at 98°C for 15 seconds. At 50°C for 30 s, the primer was completely annealed to the template; at 72°C for30 s, the primer was extended to synthesize DNA, thus completing a cycle. This cycle is repeated 25–27 times, resulting in a substantial collection of DNA fragments that have been amplified. The reaction mixture was maintain it at 72°C for 5 minutes to finish the product's extension. The products were stored at 4°C. The amplification products were electrophoresed on a 2% agarose gel. The fragments of the target were excised and then recovered using an Axygen gel recovery kit. PCR results were then measured with the Quant-iT PicoGreen dsDNA Assay Kit on a microplate reader (BioTek, FLx800). Shanghai Pesennuo Technology Co., Ltd. (Shanghai, China) was tasked with performing two 250 bp paired-end sequencing using the Illumina NovasSeq-PE300 platform, after individual quantification and pooling of equal numbers of amplicons.

2.4 Data processing

Vsearch (v2.13.4 Linux x86 64) was used for microbiome bioinformatics analysis (Edgar et al., 2011). Firstly, the original

sequence data were preprocessed by using Cutadapt to remove primer fragments and eliminate sequences that do not match the primers. Then, the fastq_ series module is used to perform concatenation, quality filtering, de-duplication, de-chimerism, and clustering on the sequence, resulting in singletons OTUs and their representative sequences. Based on the *Geobacter* abundance data and soil physicochemical properties of the samples in the Perl script, redundancy analysis (RDA) was performed using Canoco 5.1 software. We identify the factors that have the greatest influence on *Geobacter* based on the RDA result. We sort soil samples according to the most significant factors (different arable soils, different times). We utilize the R programming language to calculate the alpha-diversity of microorganisms, such as Chao1, Faith-PD, Observed-species, and Shannon index. The Derived Gene Cloud Platform (https://www.genescloud.cn/home) is used to integrate data for species random forest analysis, MetagenomeSeq analysis, and species composition analysis. Using the GS+9.0 tool, a Semi-Variance Analysis should be conducted to find the semi-variance model and parameters for the most important *Geobacter* component. ArcGIS 10.8 was used to draw a soil pH transformation map of study area, SPSS 25.0 was used to do other routine statistical analyses.

3 Results and analysis

3.1 Soil physical and chemical properties

Soil pH of arable soil in this study ranges from 4.1 to 8.2. They were divided into eight sections (<5.0, 5.0–5.5, 5.5-6.0, 6.0–6.5, 6.5-7.0, 7.0–7.5, 7.5-8.0, >8.0), with ratios of 11.1%, 5.6%, 5.5%, 9.3%, 12.9%, 20.4%, 24.1%, and 11.1%, respectively. TN content in soil was ranges from 0.09 to 0.33%. SOM content varies from 1.39 to 4.13%. TP content ranges from 0.02 to 0.13%. According to the results of XRD analysis, the iron minerals in paddy soil are mainly Hematite, Goethite, Ferrihydrite, Maghemite and Magnetite. These minerals correspond to the standard PDF cards in Jade software, and they correspond to the cards as follows: PDF#97-015-7689, PDF#97-007-7327, PDF#97-024-9048, PDF#97-009-6073, and PDF#97-016-6135.IBM content ranges from 2.13 to 16.53%. *Geobacter* abundances range from 0.11 to 1.17%. Through RDA analysis, it was found that TN, SOM, IBM, and C/N showed positive correlations with *Geobacter* and soil pH and TP showed negative relationship with *Geobacter* (Figure 2). The relative length of the vertical projection between pH and *Geobacter* is relatively long, indicating that pH is a key factor affecting the abundance of *Geobacter*. According to the ranking of the influence of *Geobacter*, the importance of physicochemical factors in paddy soil is as follows: pH>TN>TP>OM>IBM>C/N. The proportions of pH and TN to all soil physicochemical factors are 72.5% and 16.9%, respectively, and pH and TN reach a very significant level ($p<0.01$), while TN also reaches a significant level ($p<0.05$) (Table 1).

3.2 Effect of IBM content on *Geobacter* abundance

Overall, the correlation between IBM and *Geobacter* has no significance ($p>0.05$). Therefore, based on the IBM content, the samples were divided into five groups: IBM1 (5%), IBM2 (7.5%), IBM3 (9%), IBM4 (10.5%), and IBM5 (12%). We found that the greater the difference in IBM content in soil, the greater the difference in microbial abundance ($p>0.05$) (Table 2). From the results of hierarchical clustering analysis, IBM1 and IBM2 groups which have lower IBM content were relatively close in terms of species evolutionary composition, while the IBM3, IBM4 and IBM5

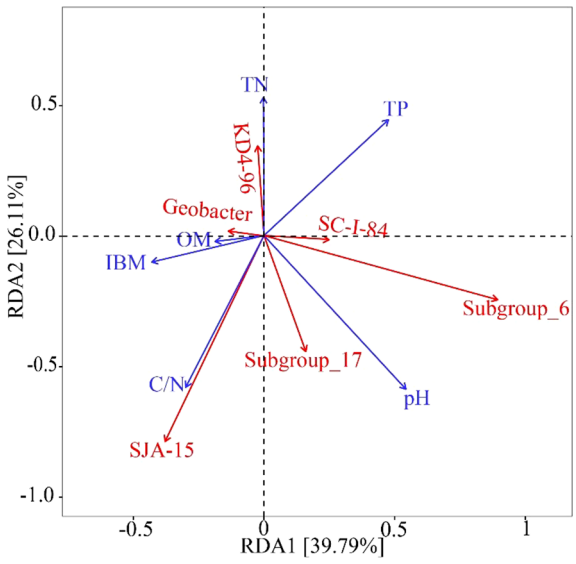

FIGURE 2
Relationship between Soil physicochemical and dominant arable soil microbial community and *Geobacter* by RDA.

10.3389/fevo.2025.1523532

TABLE 1 Contribution ranking and significance test results of soil physicochemical factors.

Name	Order of importance	Contribution %	F	P
pH	1	72.5	20.2	<0.01
TN	2	16.9	4.7	<0.05
TP	3	6.2	1.7	>0.05
OM	4	2.4	0.7	>0.05
IBM	5	1.4	0.4	>0.05
C/N	6	0.6	0.2	>0.05

groups which have a higher IBM content exhibit an interlocking state (Figure 3). For the abundance of *Geobacter*, the lower content of IBM1 and IBM2 groups showed a negative correlation with *Geobacter* abundance, while the higher content of IBM3, IBM4 and IBM5 groups showed a significant positive correlation with *Geobacter* abundance (Figure 4). These data implied that arable soil with higher IBM content has a significant impact on the relative abundance of *Geobacter*, especially when the IBM content exceeds 9%, the effect of IBM content on *Geobacter* abundance reaches a significant level.

3.3 Arable soil α-diversity analysis

Soil samples were divided into different categories by soil types (purple soil and paddy soil), soil pH (<6.5:acidic, 6.5-7.5:neutral, and >7.5:alkaline soils) and sample time (May and August). It was found that microbial diversity in arable soil increased at the genus level ($p<0.01$) with increasing pH. Soil microbial diversity shows significant differences in different sample months and soil types. The diversity of soil microorganisms is significantly higher in August than in May, and the diversity of microorganisms in purple soil is significantly lower than that in paddy soil (Figure 5).

TABLE 2 The results of the differences between microbiomes of different group.

Group1	Group2	Samples	R	P-value
IBM1	IBM2	10	0.22	0.108
IBM1	IBM3	10	0.86	0.012
IBM1	IBM4	11	0.31	0.052
IBM1	IBM5	10	0.48	0.012
IBM2	IBM3	10	1	0.011
IBM2	IBM4	11	0.47	0.011
IBM2	IBM5	10	0.98	0.008
IBM3	IBM4	11	0.52	0.008
IBM3	IBM5	10	0.99	0.011
IBM4	IBM5	11	0.89	0.004

IBM content: IBM1 (around 5%), IBM2 (around 7.5%), IBM3 (around 9%), IBM4 (around 10.5%), and IBM5 (around 12%).

3.4 Analysis of *Geobacter* occurrence abundance in arable soils

The results of random forest analysis indicate that *Geobacter* ranked 30th in importance of our sampled soil (Figure 6). Paddy soil sampled in May revealed a positive link with *Geobacter* in acidic environment, a weak correlation with a neutral environment, and a negative correlation with an alkaline environment. Paddy soils which were collected in August demonstrated a negative correlation in acidic, neutral, and alkaline environments. *Geobacter* in the purple soil collected in May and August demonstrated a weaker correlation in the neutral environment, which is negatively correlated in acidic and alkaline environments. These results indicate that *Geobacter* is more adaptable to acidic environmental in paddy soil, but in purple soil, *Geobacter* is more adaptable to neutral environment. Geostatistical analysis revealed that the pH of soil in the Sichuan Basin has decreased by an average of 0.7 over the past 40 years (Figure 7). Soil acidification phenomenon was serious especially in soil that long term affected by drainage and irrigation.

Abundance of microorganisms was greater in August than in May whether in paddy soil or purple soil. Abundance of *Geobacter* is also higher in August than in May. In paddy soil, the abundance of *Geobacter* reaches 0.83% and decreased with increasing pH. In purple soil, the abundance of *Geobacter* first increases and then decreases with the increase of pH, and *Geobacter* prefer neutral purple soil, its maximum abundance reaches 0.68% (Figure 8). Further analysis through metagenomeSeq revealed that there was a significant upregulation of *Geobacter* in paddy soil in August compared to May, and its abundance ranked among the top 10 at the genus level (Figure 9). However, there was no significant difference in *Geobacter* in purple soil. Through the analysis of the content changes of non-stable crystal Ferrihydrite in different soil types and months, it was found that the content of ferrihydrite in paddy soil in August was lower than that in May, while this trend was not observed in purple soil (Table 3).

4 Discussions

4.1 Effects of soil physicochemical properties on *Geobacter* abundance in arable soil

pH had a negative correlation with *Geobacter* abundance and its contribution reached 72.5% ($p<0.01$). This result mutually agree with another result which demonstrated that *Geobacter* abundance declined from 2.89 percent to 0.9 percent in paddy soils as pH increased (Li et al., 2019). *Geobacter* can utilize a variety of substrates for respiratory metabolism that the best growth pH range for *Geobacter* is between 5.5 and 7.0, which corresponds to

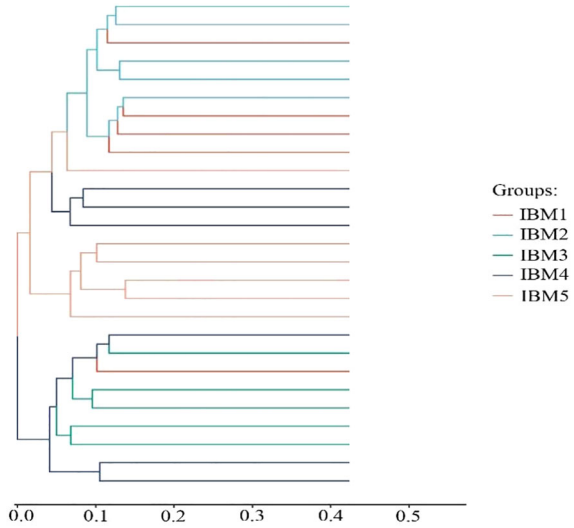

FIGURE 3
Hierarchical clustering tree diagram, in which samples are clustered according to their similarity. The shorter the branch length between samples, the more similar the two samples are. IBM content: IBM1 (around 5%), IBM2 (around 7.5%), IBM3 (around 9%), IBM4 (around 10.5%), and IBM5 (around 12%).

a neutral and acidic environment (Straub and Buchholz-Cleven, 2001; Wang et al., 2021; Xu et al., 2019).

IBM is a receptor for *Geobacter* to directly transfer electrons through conductive pili. When IBM is Added under ideal cultivation conditions, an increase in the abundance of *Geobacter* can be observed, which is mainly caused by Magnetite that is the main content of IBM (Kato et al., 2010; Zhang et al., 2020). Hematite, Goethite, and Maghemite have lower transfer efficiency than direct conductors when accepting electrons and transferring them to end acceptors. At the same time, these iron containing semiconductor minerals accept photoelectrons catalyzed by sunlight under natural conditions. They accept electrons produced by *Geobacter* while reacting with *Geobacter* (Lu et al., 2012). When the content of IBM is low, it often cannot reach the level that affects *Geobacter* abundance (Qiu et al., 2019). This may be the reason why IBM content did not have a widespread impact on the abundance of *Geobacter* in the topsoil. Therefore, we divided the IBM content in our study and found that when the IBM content exceeded 9%, it had a positive correlation with the abundance of *Geobacter*. Due to the ubiquitous presence of IBM in the topsoil, its involvement in the study of *Geobacter* mediated energy cycling of other substances cannot be ignored.

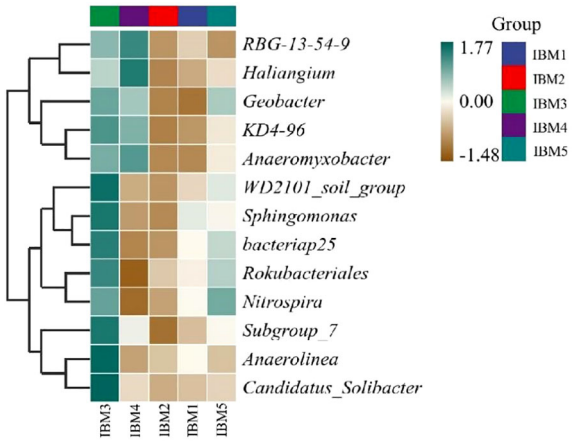

FIGURE 4
Correlation analysis of heat maps, the shorter the branch length between the strains, the more similar the taxonomic level between the strains, heatmap showing how these species abundances are correlated within each group, the ordinate on the right is the taxon name at the genus level.

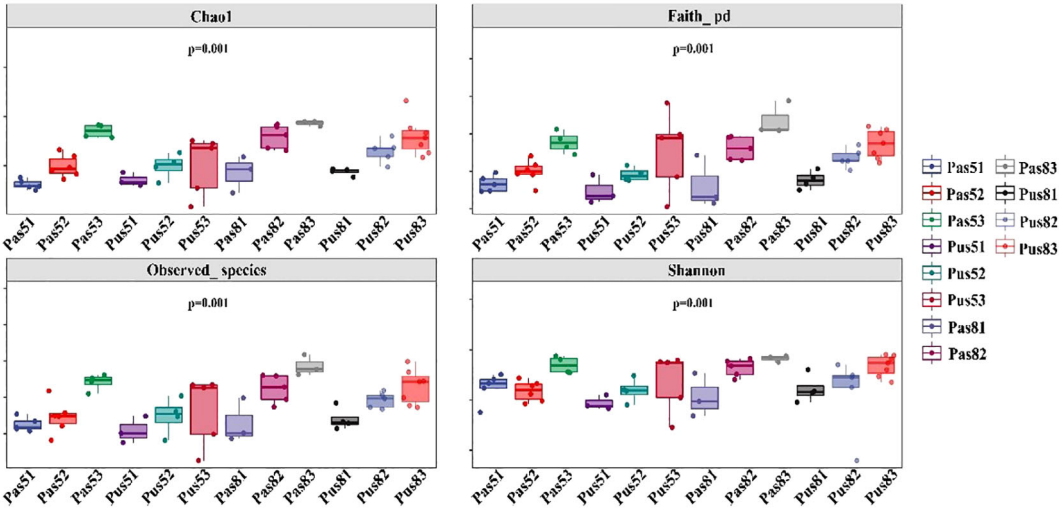

FIGURE 5
The results of α-diversity. The horizontal axis is the grouping label (Pas: soil collected from paddy soil; Pus:soil collected from purple soil; 5:May; 8: August; 1:acidic; 2: neutral; 3: alkaline), and the verticle axis is the corresponding alpha diversity index value(Includes: Chao1, Faith_pd, Observed_specics, Shannon).

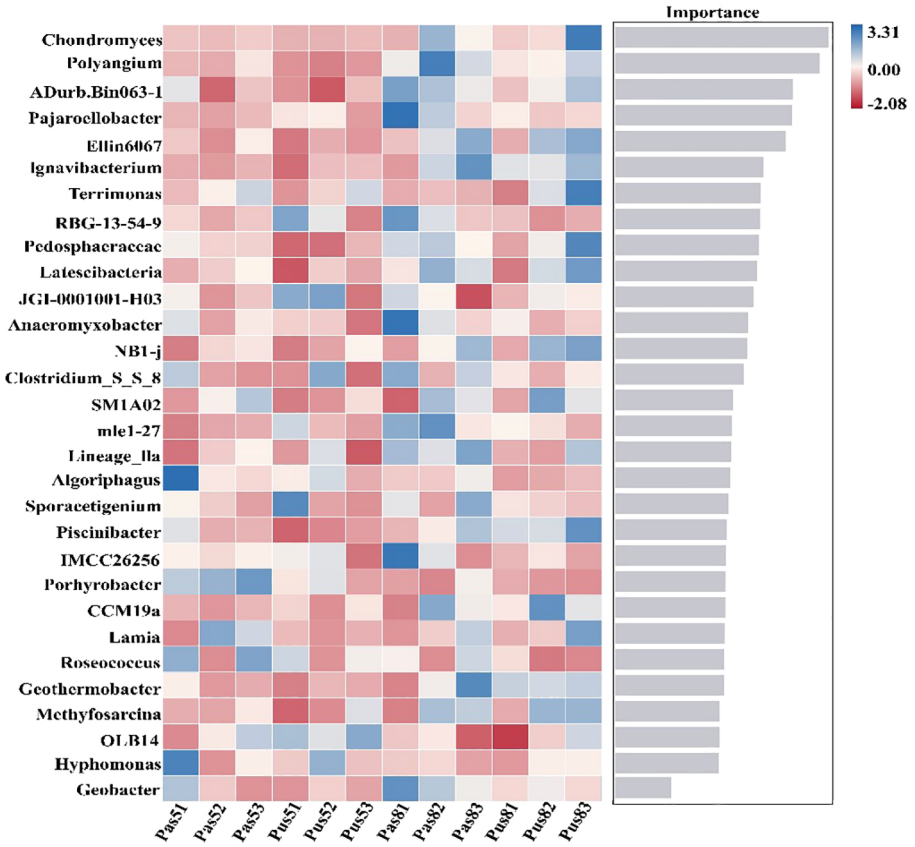

FIGURE 6
The results of species random forest analysis. The horizontal axis of the histogram is the score value of the importance of the species to the classifier model (Pas: soil collected from paddy soil; Pus:soil collected from purple soil; 5:May; 8: August; 1:acidic; 2: neutral; 3: alkaline). The verticle axis is the taxon name at the genus level, heatmap showing the abundance distribution of these species in each group, from top to bottom, species are of decreasing importance to the model.

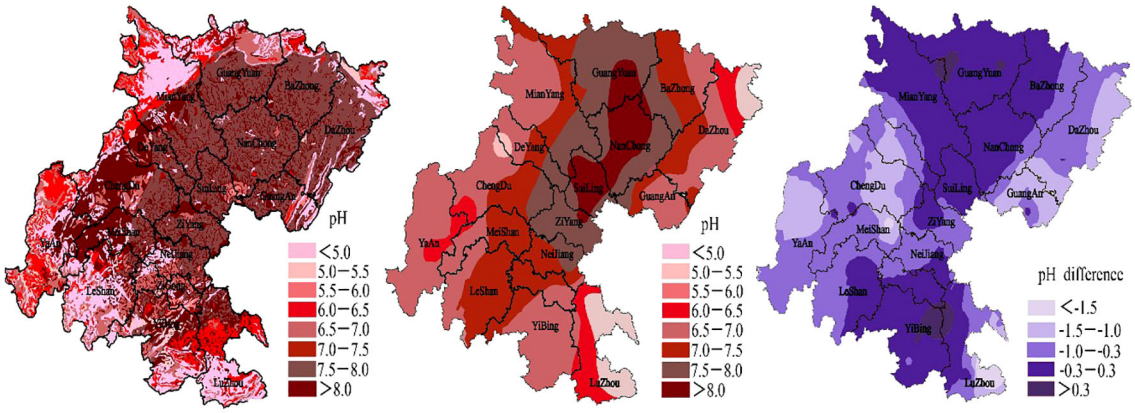

FIGURE 7
Variation of pH in arable soil in the Sichuan Basin for 40 years. **(a)** pH distribution map in 1980, **(b)** pH distribution map in 2020, **(c)** pH difference between two periods.

4.2 *Geobacter* abundance various with pH and IBM content in different soil type

Under the dual effects of human activities and natural soil formation, paddy soils, especially winter paddy fields in the Sichuan Basin, have long been in a state of flooding and hypoxia (Xu et al., 2020). Due to differences in the soil formation status and utilization methods of the plow layer, even with the same tillage measures, differences in soil microbial abundance can still be observed (Yan et al., 2019). The abundance of *Geobacter* in paddy soil under long-term flooding conditions is significantly higher than that in purple soil. The abundance of *Geobacter* in acidic paddy soil and neutral purple soil is higher than that in cultivated soil during the same period, which may be related to the acidification of paddy soil. In the past 40 years, the average pH decrease in cultivated soil in the Sichuan Basin has reached 0.7 units, which has led to *Geobacter* tending towards neutral and acidic environments. There is research confirming that small changes in water balance can lead to a steep transition from alkaline to acidic soil. During the continuous drainage and irrigation process, alkaline cations and Si in the soil are completely lost, while Al^{3+} loss is relatively small, resulting in a decrease in soil pH. Finally, *Geobacter* in paddy soil tends to adapt more to acidic environments (Chadwick et al., 2003;

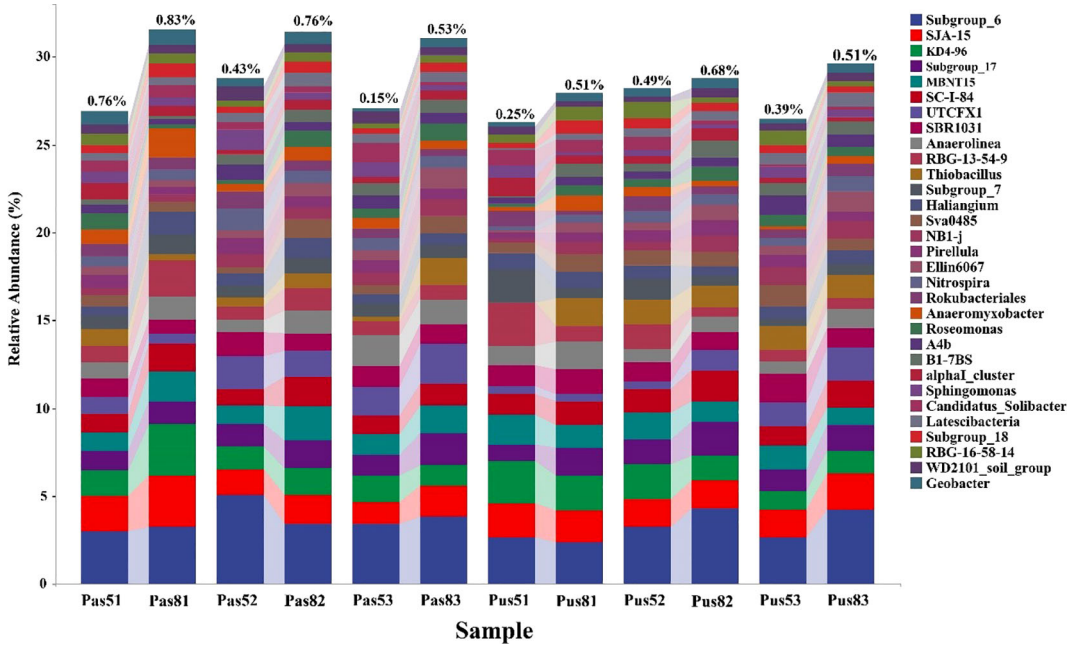

FIGURE 8
Species composition analysis, the horizontal axis is the grouping label (Pas: soil collected from paddy soil; Pus:soil collected from purple soil; 5:May; 8: August; 1:acidic; 2: neutral; 3: alkaline), and the verticle axis is the relative abundance of each taxon at the genus level. The abundance of *Geobacter* is at the top of each grouping scheme and the abundance value is marked.

Slessarev et al., 2016). As a primary fertile purple soil, although short-term irrigation is carried out during the rice planting period, the linear relationship between soil leaching coefficient and soil renewal always maintains the relative stability of soil pH in the plow layer (Li et al., 2010; Wang and Zhu, 2011).

Overall, the abundance of *Geobacter* in paddy soil and purple soil showed a higher occurrence in August than in May, which can be attributed to the fact that the temperature in August was higher than that in May in the Sichuan Basin. This is because the optimal growth temperature for *Geobacter* is 30-35 °C, which is conducive to improving its electron transfer efficiency (Bannister et al., 2017; Heidrich et al., 2018; Xiao et al., 2021). On the other hand, in May, rice entered the greening period, and the flooded environment caused by a large amount of irrigation led to an upward trend in soil pH. In August, rice entered the maturity period, and the drainage process caused a linear decrease in soil pH (Ding et al., 2019). In addition, after the drainage of paddy soil, the soil redox potential continues to increase, and the presence of the differentiated reduction product Fe^{2+} is very conducive to the transformation of oxides from amorphous to crystalline form (Minamikawa and Sakai, 2006; Zachara et al., 2002). Some studies has found that Fe^{2+}oxidation can lead to a decrease in soil pH (Hall and Silver, 2013). At the same time, the IBM content will increase because under stable oxygen-containing conditions, Fe^{2+} rapidly re oxidizes to form Ferrihydrate, which then slowly transforms into thermodynamically more stable hematite or goethite (Vogelsang et al., 2016). Overall, these factors better explain the significantly higher abundance of *Geobacter* in paddy soil in August compared to May.

5 Conclusion

The abundance of *Geobacter* in paddy soil and purple soil of the Sichuan Basin was analyzed using 16sRNA high-throughput

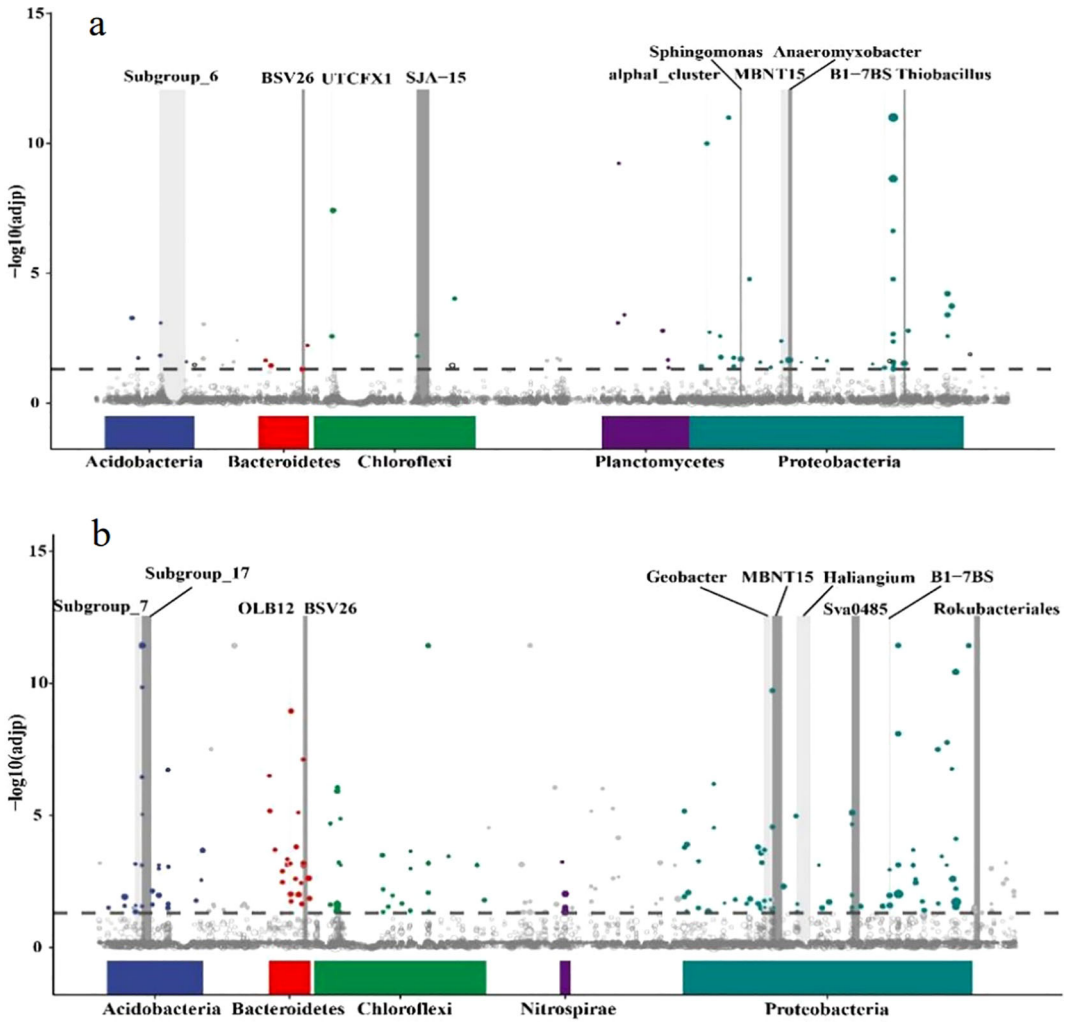

FIGURE 9
Manhattan plot, **(a)**: paddy soil, **(b)**: purple soil. The bottom of the horizontal axis represents the distribution characteristics at the gate level; the vertical axis is the -log10 (adjp) value, the higher the position of the dot, the more significant the difference, the horizontal dotted line is a significant difference line, above the dotted line means there is a significant difference ($p<0.05$), the dotted line The following indicates no significant difference; bars represent genera and species with significant differences at the genus level.

TABLE 3 Distribution ratio of iron oxides in different soil types and sampling times.

	Pas5	Pas8	Pus5	Pus8
Hematite	4.53 ± 0.34	4.46 ± 0.66	4.43 ± 0.49	4.45 ± 0.45
Goethite	1.13 ± 0.16	1.13 ± 0.31	1.05 ± 0.23	0.98 ± 0.21
Ferrihydrite	2.91 ± 0.28	2.16 ± 0.55	2.08 ± 0.41	2.48 ± 0.38
Maghemite	1.21 ± 0.14	1.19 ± 0.28	1.41 ± 0.21	1.49 ± 0.19
Magnetite	0.24 ± 0.04	0.21 ± 0.07	0.25 ± 0.05	0.21 ± 0.05
Total	10.02 ± 0.60	9.13 ± 1.16	9.22 ± 0.87	9.60 ± 0.80

Pas5: soil collected from paddy soil at May; Pas8: soil collected from paddy soil at August; Pus5: soil collected from purple soil at May; Pus8: soil collected from purple soil at August.

sequencing technology, and it was found that the abundance of *Geobacter* was correlated with soil pH and IBM content. There is a negative correlation between soil pH and *Geobacter* abundance, with a contribution of up to 72.5%. When the IBM content in the soil exceeds 9%, it will have a positive impact on the abundance of *Geobacter*. According to the grouping of different pH levels, soil types, and sample months, it was found that *Geobacter* in paddy soil have a higher abundance in acidic environments, while *Geobacter* in purple soil seems to be more adaptable to neutral environments. Further analysis suggests that long-term irrigation and drainage lead to soil acidification may be the cause of the differences. The average pH decrease of cultivated soil in the Sichuan Basin over the past 40 years is 0.7 unit, which may be an important reason for *Geobacter*'s tendency towards neutral and acidic environments. Overall, the abundance of *Geobacter* in paddy soil and purple soil increased significantly in August compared to May, which is related to hydrothermal conditions and the conversion of iron oxides under different moisture conditions. Microbial reduction of iron oxide minerals as an important component of iron biogeochemical cycling is gradually being recognized, and the results of this study will contribute to deepening the interaction between *Geobacter* and IBM in acidified soils and their impact on carbon dynamics.

Data availability statement

The original contributions presented in the study are included in the article/supplementary material. Further inquiries can be directed to the corresponding authors.

Author contributions

YB: Funding acquisition, Writing – original draft. QD: Writing – review & editing. JG: Writing – review & editing. WF: Writing – review & editing. JY: Writing – review & editing. FW: Writing – review & editing. JH: Funding acquisition, Writing – review & editing. RZ: Funding acquisition, Writing – review & editing. GY: Funding acquisition, Supervision, Writing – review & editing.

Funding

The author(s) declare that financial support was received for the research and/or publication of this article. This work was supported by the Sichuan Science and Technology Program (grant number 2023NSFSC0758), National Natural Science Foundation of China (grant number 42430715), the National Key R&D Program of China (grant number 2022YFD2300600, 2023YFD2301903).

Conflict of interest

The authors declare that the research was conducted in the absence of any commercial or financial relationships that could be construed as a potential conflict of interest.

Generative AI statement

The author(s) declare that no Generative AI was used in the creation of this manuscript.

Publisher's note

All claims expressed in this article are solely those of the authors and do not necessarily represent those of their affiliated organizations, or those of the publisher, the editors and the reviewers. Any product that may be evaluated in this article, or claim that may be made by its manufacturer, is not guaranteed or endorsed by the publisher.

References

Alikhan, N.-F., Petty, N. K., Ben Zakour, N. L., and Beatson, S. A. (2011). BLAST Ring Image Generator (BRIG): simple prokaryote genome comparisons. *BMC Genomics* 12, 1–10. doi: 10.1186/1471-2164-12-402

Bannister, D., Herzog, M., Graf, H.-F., Hosking, J. S., and Short, C. A. (2017). An assessment of recent and future temperature change over the Sichuan Basin, China, using CMIP5 climate models. *J. Climate.* 30, 6701–6722. doi: 10.1175/JCLI-D-16-0536.1

Caccavo, J. F., Lonergan, D. J., Lovley, D. R., Davis, M., Stolz, J. F., and McInerney, M. J. (1994). Geobacter sulfurreducens sp. nov., a hydrogen-and acetate-oxidizing dissimilatory metal-reducing microorganism. *Appl. Environ. Microbiol.* 60, 3752–3759. doi: 10.1128/aem.60.10.3752-3759.1994

Chadwick, O. A., Gavenda, R. T., Kelly, E. F., Ziegler, K., Olson, C. G., Elliott, W. C., et al. (2003). The impact of climate on the biogeochemical functioning of volcanic soils. *Chem. Geology.* 202, 195–223. doi: 10.1016/j.chemgeo.2002.09.001

Chung, F. H. (1974). Quantitative interpretation of X-ray diffraction patterns of mixtures. II. Adiabatic principle of X-ray diffraction analysis of mixtures. *J. Appl. Crystallography.* 7, 526–531. doi: 10.1107/S0021889874010387

Ding, C., Du, S., Ma, Y., Li, X., Zhang, T., and Wang, X. (2019). Changes in the pH of paddy soils after flooding and drainage: modeling and validation. *Geoderma* 337, 511–513. doi: 10.1016/j.geoderma.2018.10.012

Dubey, A., Malla, M. A., Khan, F., Chowdhary, K., Yadav, S., Kumar, A., et al. (2019). Soil microbiome: a key player for conservation of soil health under changing climate. *Biodiversity Conserv.* 28, 2405–2429. doi: 10.1007/s10531-019-01760-5

Edgar, R. C., Haas, B. J., Clemente, J. C., Quince, C., and Knight, R. (2011). UCHIME improves sensitivity and speed of chimera detection. *Bioinformatics* 27, 2194–2200. doi: 10.1093/bioinformatics/btr381

Fierer, N. (2017). Embracing the unknown: disentangling the complexities of the soil microbiome. *Nat. Rev. Microbiol.* 15, 579–590. doi: 10.1038/nrmicro.2017.87

Franke-Whittle, I. H., Manici, L. M., Insam, H., and Stres, B. (2015). Rhizosphere bacteria and fungi associated with plant growth in soils of three replanted apple orchards. *Plant Soil.* 395, 317–333. doi: 10.1007/s11104-015-2562-x

Hall, S. J., and Silver, W. L. (2013). Iron oxidation stimulates organic matter decomposition in humid tropical forest soils. *Global Change Biol.* 19, 2804–2813. doi: 10.1111/gcb.2013.19.issue-9

Harris, W., and Norman White, G. (2008). X-ray diffraction techniques for soil mineral identification. *Methods Soil Anal. Part 5—Mineralogical Methods* 5, 81–115. doi: 10.2136/sssabookser5.5.c4

Heidrich, E., Dolfing, J., Wade, M., Sloan, W., Quince, C., and Curtis, T. (2018). Temperature, inocula and substrate: Contrasting electroactive consortia, diversity and performance in microbial fuel cells. *Bioelectrochemistry* 119, 43–50. doi: 10.1016/j.bioelechem.2017.07.006

Huang, J., Sheng, X., He, L., Huang, Z., Wang, Q., and Zhang, Z. (2013). Characterization of depth-related changes in bacterial community compositions and functions of a paddy soil profile. *FEMS Microbiol. letters.* 347, 33–42. doi: 10.1111/fml.2013.347.issue-1

Jansson, J. K., and Hofmockel, K. S. (2020). Soil microbiomes and climate change. *Nat. Rev. Microbiol.* 18, 35–46. doi: 10.1038/s41579-019-0265-7

Kato, S., Hashimoto, K., and Watanabe, K. (2012). Methanogenesis facilitated by electric syntrophy via (semi) conductive iron-oxide minerals. *Environ. Microbiol.* 14, 1646–1654. doi: 10.1111/j.1462-2920.2011.02611.x

Kato, S., Hashimoto, K., and Watanabe, K. (2013). Iron-oxide minerals affect extracellular electron-transfer paths of Geobacter spp. *Microbes environments* 28, 141–148. doi: 10.1264/jsme2.ME12161

Kato, S., Nakamura, R., Kai, F., Watanabe, K., and Hashimoto, K. (2010). Respiratory interactions of soil bacteria with (semi) conductive iron-oxide minerals. *Environ. Microbiol.* 12, 3114–3123. doi: 10.1111/j.1462-2920.2010.02284.x

Kramer, S., Marhan, S., Haslwimmer, H., Ruess, L., and Kandeler, E. (2013). Temporal variation in surface and subsoil abundance and function of the soil microbial community in an arable soil. *Soil Biol. Biochem.* 61, 76–85. doi: 10.1016/j.soilbio.2013.02.006

Kunapuli, U., Jahn, M. K., Lueders, T., Geyer, R., Heipieper, H. J., and Meckenstock, R. U. (2010). Desulfitobacterium aromaticivorans sp. nov. and Geobacter toluenoxydans sp. nov., iron-reducing bacteria capable of anaerobic degradation of monoaromatic hydrocarbons. *Int. J. Systematic Evolutionary Microbiol.* 60, 686–695. doi: 10.1099/ijs.0.003525-0

Lei, C., Qi, Q., Fu, Y., Jiang, L., and Liang, Q. (2022). Analysis on mechanism of China's grain production development and evolution from 1985 to 2019. *IEEE Access.* 10, 43221–43234. doi: 10.1109/ACCESS.2022.3165189

Li, X., Ding, L., Li, X., and Zhu, Y. (2020). Abundance, diversity, and structure of Geobacteraceae community in paddy soil under long-term fertilization practices. *Appl. Soil Ecology.* 153, 103577. doi: 10.1016/j.apsoil.2020.103577

Li, S., Li, Z., Feng, X., Zhou, F., Wang, J., and Li, Y. (2021). Effects of biochar additions on the soil chemical properties, bacterial community structure and rape growth in an acid purple soil. *Plant Soil Environment.* 67, 121–129. doi: 10.17221/390/2020-PSE

Li, H., Su, J.-Q., Yang, X.-R., Zhou, G.-W., Lassen, S. B., and Zhu, Y.-G. (2019). RNA stable isotope probing of potential Feammox population in paddy soil. *Environ. Sci. technology.* 53, 4841–4849. doi: 10.1021/acs.est.8b05016

Li, T., and Zhou, Q. (2020). The key role of Geobacter in regulating emissions and biogeochemical cycling of soil-derived greenhouse gases. *Environ. Pollution*. 266, 115135. doi: 10.1016/j.envpol.2020.115135

Li, L., Zhou, Z., and Liu, G. (2010). Model-based estimation and field measurement of purple soil formation rate. *Acta Pedologica Sinica.* 47, 393–400. doi: 10.11766/trxb200807150302

Liu, L., Zhu, K., Wurzburger, N., and Zhang, J. (2020). Relationships between plant diversity and soil microbial diversity vary across taxonomic groups and spatial scales. *Ecosphere* 11, e02999. doi: 10.1002/ecs2.v11.1

Lovley, D. R. (2022). Microbe Profile: Geobacter metallireducens: a model for novel physiologies of biogeochemical and technological significance. *Microbiology* 168, 001138. doi: 10.1099/mic.0.001138

Lovley, D. R., Giovannoni, S. J., White, D. C., Champine, J. E., Phillips, E., Gorby, Y. A., et al. (1993). Geobacter metallireducens gen. nov. sp. nov., a microorganism capable of coupling the complete oxidation of organic compounds to the reduction of iron and other metals. *Arch. Microbiol.* 159, 336–344. doi: 10.1007/BF00290916

Lovley, D. R., Ueki, T., Zhang, T., Malvankar, N. S., Shrestha, P. M., Flanagan, K. A., et al. (2011). Geobacter: the microbe electric's physiology, ecology, and practical applications. *Adv. microbial Physiol.* 59, 1–100. doi: 10.1016/B978-0-12-387661-4.00004-5

Lu, A., Li, Y., Jin, S., Wang, X., Wu, X.-L., Zeng, C., et al. (2012). Growth of non-phototrophic microorganisms using solar energy through mineral photocatalysis. *Nat. Commun.* 3, 1–8. doi: 10.1038/ncomms1768

Luo, G., Li, L., Friman, V.-P., Guo, J., Guo, S., Shen, Q., et al. (2018). Organic amendments increase crop yields by improving microbe-mediated soil functioning of agroecosystems: A meta-analysis. *Soil Biol. Biochem.* 124, 105–115. doi: 10.1016/j.soilbio.2018.06.002

Methe, B., Nelson, K. E., Eisen, J. A., Paulsen, I. T., Nelson, W., Heidelberg, J., et al. (2003). Genome of Geobacter sulfurreducens: metal reduction in subsurface environments. *Science* 302, 1967–1969. doi: 10.1126/science.1088727

Minamikawa, K., and Sakai, N. (2006). The practical use of water management based on soil redox potential for decreasing methane emission from a paddy field in Japan. *Agriculture Ecosyst. environment.* 116, 181–188. doi: 10.1016/j.agee.2006.02.006

Prakash, O., Gihring, T. M., Dalton, D. D., Chin, K.-J., Green, S. J., Akob, D. M., et al. (2010). Geobacter daltonii sp. nov., an Fe (III)-and uranium (VI)-reducing bacterium isolated from a shallow subsurface exposed to mixed heavy metal and hydrocarbon contamination. *Int. J. systematic evolutionary Microbiol.* 60, 546–553. doi: 10.1099/ijs.0.010843-0

Qiu, C., Feng, Y., Wu, M., Zhang, J., Chen, X., and Li, Z. (2019). NanoFe3O4 accelerates methanogenic straw degradation in paddy soil enrichments. *Appl. Soil Ecology.* 144, 155–164. doi: 10.1016/j.apsoil.2019.07.015

Ran, W., and Xinyue, Z. (2018). Spatial structure and elements of boundaries of traditional" Shan-Shui cities" in the Sichuan Basin. *J. Landscape Res.* 10, 78–82. doi: 10.16785/jjssn 1943-989x.2018.4.017

Rengel, Z., and Marschner, P. (2005). Nutrient availability and management in the rhizosphere: exploiting genotypic differences. *New Phytologist*. 168, 305–312. doi: 10.1111/j.1469-8137.2005.01558.x

Rotaru, A.-E., Calabrese, F., Stryhanyuk, H., Musat, F., Shrestha, P. M., Weber, H. S., et al. (2018). Conductive particles enable syntrophic acetate oxidation between Geobacter and Methanosarcina from coastal sediments. *MBio* 9, e00226–e00218. doi: 10.1128/mBio.00226-18

Slessarev, E., Lin, Y., Bingham, N., Johnson, J., Dai, Y., Schimel, J., et al. (2016). Water balance creates a threshold in soil pH at the global scale. *Nature* 540, 567–569. doi: 10.1038/nature20139

Straub, K. L., and Buchholz-Cleven, B. (2001). Geobacter bremensis sp. nov. and Geobacter pelophilus sp. nov., two dissimilatory ferric-iron-reducing bacteria. *Int. J. Systematic Evolutionary Microbiol.* 51, 1805–1808. doi: 10.1099/00207713-51-5-1805

Vogelsang, V., Kaiser, K., Wagner, F., Jahn, R., and Fiedler, S. (2016). Transformation of clay-sized minerals in soils exposed to prolonged regular alternation of redox conditions. *Geoderma* 278, 40–48. doi: 10.1016/j.geoderma.2016.05.013

Wang, J., Deng, H., Wu, S.-S., Deng, Y.-C., Liu, L., Han, C., et al. (2019). Assessment of abundance and diversity of exoelectrogenic bacteria in soil under different land use types. *Catena* 172, 572–580. doi: 10.1016/j.catena.2018.09.028

Wang, T., and Zhu, B. (2011). Nitrate loss via overland flow and interflow from a sloped farmland in the hilly area of purple soil, China. *Nutrient Cycling Agroecosystems.* 90, 309–319. doi: 10.1007/s10705-011-9431-7

Wang, T., Zhu, G., Kuang, B., Jia, J., Liu, C., Cai, G., et al. (2021). Novel insights into the anaerobic digestion of propionate via Syntrophobacter fumaroxidans and Geobacter sulfurreducens: process and mechanism. *Water Res.* 200, 117270. doi: 10.1016/j.watres.2021.117270

Wardle, D., Yeates, G., Nicholson, K., Bonner, K., and Watson, R. (1999). Response of soil microbial biomass dynamics, activity and plant litter decomposition to agricultural intensification over a seven-year period. *Soil Biol. Biochem.* 31, 1707–1720. doi: 10.1016/S0038-0717(99)00090-5

Xiao, L., Li, J., Lichtfouse, E., Li, Z., Wang, Q., and Liu, F. (2021). Augmentation of chloramphenicol degradation by Geobacter-based biocatalysis and electric field. *J. Hazardous Materials.* 410, 124977. doi: 10.1016/j.jhazmat.2020.124977

Xu, Z., Masuda, Y., Itoh, H., Ushijima, N., Shiratori, Y., and Senoo, K. (2019). Geomonas oryzae gen. nov., sp. nov., Geomonas edaphica sp. nov., Geomonas ferrireducens sp. nov., Geomonas terrae sp. nov., Four Ferric-Reducing Bacteria Isolated From Paddy Soil, and Reclassification of Three Species of the Genus Geobacter as Members of the Genus Geomonas gen. nov. *Front. Microbiol.* 10, 2201. doi: 10.3389/fmicb.2019.02201

Xu, P., Zhou, W., Jiang, M., Shaaban, M., Zhou, M., Zhu, B., et al. (2020). Conversion of winter flooded rice paddy planting to rice-wheat rotation decreased methane emissions during the rice-growing seasons. *Soil Tillage Res.* 198, 104490. doi: 10.1016/j.still.2019.104490

Yan, S., Niu, Z., Zhang, A., Yan, H., Zhang, H., He, K., et al. (2019). Biochar application on paddy and purple soils in southern China: soil carbon and biotic activity. *R. Soc. Open science.* 6, 181499. doi: 10.1098/rsos.181499

Zachara, J. M., Kukkadapu, R. K., Fredrickson, J. K., Gorby, Y. A., and Smith, S. C. (2002). Biomineralization of poorly crystalline Fe (III) oxides by dissimilatory metal reducing bacteria (DMRB). *Geomicrobiology J.* 19, 179–207. doi: 10.1080/01490450252864271

Zhang, F., Battaglia-Brunet, F., Hellal, J., Joulian, C., Gautret, P., and Motelica-Heino, M. (2020). Impact of Fe (III)(oxyhydr) oxides mineralogy on iron solubilization and associated microbial communities. *Front. Microbiol.* 11, 571244. doi: 10.3389/fmicb.2020.571244

Zheng, T., Deng, Y., Wang, Y., Jiang, H., O'Loughlin, E. J., Flynn, T. M., et al. (2019). Seasonal microbial variation accounts for arsenic dynamics in shallow alluvial aquifer systems. *J. hazardous materials.* 367, 109–119. doi: 10.1016/j.jhazmat.2018.12.087

Zhu, J., Yan, X., Zhou, L., Li, N., Liao, C., and Wang, X. (2022). Insight of bacteria and archaea in Feammox community enriched from different soils. *Environ. Res.* 203, 111802. doi: 10.1016/j.envres.2021.111802